Optical transmission of photonic crystal structures formed by dielectric cylinders: Evidence for non-negative refraction

Chao-Hsien Kuo and Zhen Ye*
Wave Phenomena Laboratory, Department of Physics, National Central University, Chungli, Taiwan, Republic of China
(Received 17 October 2003; published 16 November 2004)

By a rigorous numerical simulation based on the standard multiple scattering theory, we investigate optical transmission in photonic crystal structures, formed from dielectric cylinders embedded in parallel in a uniform medium. In contrast to previous conjectures, the results indicate that the imaging effect of a flat photonic crystal slab, which has been interpreted as a signature of negative refractive effects, is caused by a tunneling or self-guiding effect in the presence of partial band gaps.

DOI: 10.1103/PhysRevE.70.056608 PACS number(s): 42.30.Wb, 78.20.Ci, 73.20.Mf, 78.66.Bz

Ever since the proposal that a perfect lens can be realized by the so-called left-handed material (LHM) or negative refraction index material (NRIM), a conceptual material first introduced by Veselago many years ago [1], the research on such a superlens and LHM has been skyrocketing in the midst of much debate. A great body of literature has been and continues to be generated.

Although there are a few recent challenges with regard to the concept of LHM or relevant negative refraction effects [2–7], the mainstream consensus has been that some indications of negative refraction effects are affirmative. Support from both theoretical and experimental perspectives has been reported [8–11]. Among them, a major portion of research has been on generating the negative refraction effects by photonic crystals (PCS) [8,10–13]. For example, the authors in [8] demonstrated an unusual focused image when electromagnetic waves propagate through a rectangular slab of photonic crystal formed by regular arrays of dielectric cylinders in a uniform medium. Since the image could not be explained in the framework of the usual positive refraction, the authors have attributed the cause to the all-angle negative refraction, a concept conceived from LHMs.

Upon inspection, we found that the claim of previous evidence for negative refraction effects generated by photonic crystals might be questionable. In fact, we found that the unusual imaging or the apparent abnormal refraction that has been thought to be a negative refraction effect can be well explained in terms of the partial gaps revealed by the photonic crystals. In the present paper, we show some results to support our point of view.

Here we consider the transmission of photonic waves in photonic crystals. To be more comparable with published results, we will use the photonic crystal structures which have been commonly adopted in previous simulations, such as those in [8]. Unlike most previous FDTD simulations, we will employ the standard multiple scattering theory (MST) to compute the propagation and scattering of the waves. This theory is exact and was first formulated systematically by Twersky [14], after which it was reformulated and applied to optical, sonic and water wave problems [15–17]. In guiding our discussion, the band structures of the photonic crystals will be computed by the conventional plane-wave expansion method. As we will see, an image can indeed appear across a rectangular slab of photonic crystals. But this image is not due to the negative refraction effect, rather it is caused by guided propagation in the presence of a partial gap in the corresponding band structures.

The systems we consider are two-dimensional arrays of parallel dielectric cylinders placed in a unform medium, which we assume to be air. Consider an arbitrary array of identical dielectric cylinders placed in air. The solution for the wave scattering or propagation through such an array can be obtained by the multiple scattering theory. The essence of the theory is summarized as follows. In response to the incident wave from the source and the scattered waves from other scatterers, each scatterer will scatter waves repeatedly, and the scattered waves can be expressed in terms of a modal series of partial waves. Considering these scattered waves as an incident wave to other scatterers, a set of coupled equations can be formulated and computed rigorously. The total wave at any spatial point is the sum of the direct wave from the source and the scattered waves from all scatterers. The intensity of the waves is represented by the modulus of the wave field. In actual computation, the maximum number of modes will depends on the frequency. In the present simulation, the number of modes is up to seven, thus making the results convergent. For details about MST, refer to Ref. [16].

For brevity, we only consider the E-polarized waves, that is, the electric field is kept parallel to the cylinders. The following parameters are used in the simulation. (1) The dielectric constant of the cylinders is 14, and the cylinders are arranged in air to form a square lattice. (2) The lattice constant is a and the radius of the cylinders is $0.3a$; in the computation, all lengths are scaled by the lattice constant.

First we consider the propagation of photonic waves through a rectangular slab of an array of dielectric cylinders, by analogy with those shown in [8]. The slab width (vertical) equals $40\sqrt{2}$, and the length (horizontal) is $3\sqrt{2}$. The source is placed at 0.35 from the left side of the lattice—the geometry can be referred to in Fig. 1. The incident wave propagates along the ΓM, i.e., the [1,1] direction.

Figure 1 shows the imaging fields and the band structure. In the left panel, the band structure is plotted and the quali-

*Electronic address: zhen@phy.ncu.edu.tw

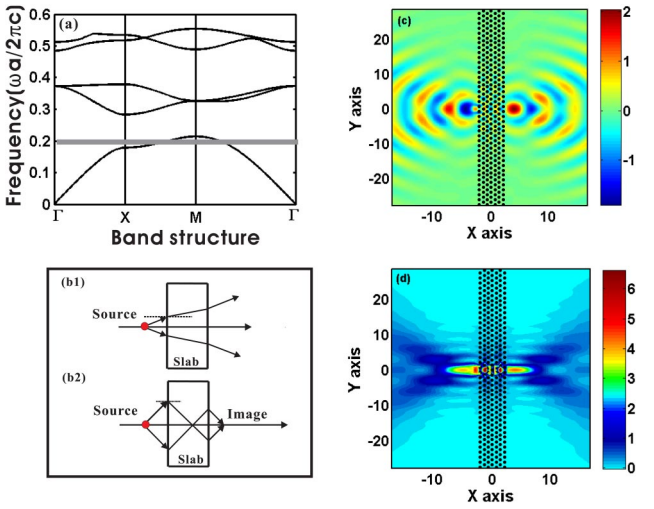

FIG. 1. (Color online) Left panel: (a) Band structure; the shaded horizontal region indicates the frequency range within which the frequency band is everywhere convex; (b) the conceptual diagrams showing the conventional and negative refraction scenarios. Right panel shows the imaging fields across the slab: (c) the real part of the electric field; (d) the intensity field, i.e., the modulus of the electric field. Hereafter, the dark circles denote the cylinders. The source is on the left-hand side of the slab.

tative features are similar to that obtained for a square array of alumina rods in air. The horizontal darkened area refers to the region in which the frequency band is convex. This frequency range, called the AANR region in [8], has been regarded as being essential for all angle negative refraction [9]. Plotted in the right panel are the real part as well as the modulus of the total electrical field. Hereafter, the spatial resolution for the image is about 0.2 to 0.3 of the lattice constant. The frequency is chosen at $0.192\times 2\pi c/a$ which is nearly at the middle of the AANR region. Here, we indeed observe a focused image point on the right-hand side of the slab. This imaging effect is more apparent in the plot of the real part of the field, and is essentially the same as that observed by the FDTD simulation for the similar photonic crystals [8]. Moreover, such a focusing effect is persistent for frequencies within the shaded area and also a regime just outside this area [18]; we note here that the data interpretation in Ref. [18] is not appropriate.

Such a focused imaging by a slab of materials is impossible in the framework of the usual positive refraction. The reason is as follows. At the frequency considered, the lattice constant is much smaller than the wavelength of the incident wave (i.e., the ratio amounts to 0.192). Therefore, the transmitted wave might be expected to be insensitive to the detailed structure of the media, that is, homogenization might be expected. Therefore, the slab may be regarded as an effective medium with an effective refractive index. If the refractive index were positive, the transmitted waves would diverge after crossing the slab. As such, no image could possibly be focused on the other side of the slab. This scenario is depicted by Fig. 1(b1). Thus the focused image shown by Fig. 1(c) cannot be explained in terms of the positive refraction. In the literature, such a focused imaging effect has been regarded as the onset of negative refraction, expected for LHMs. Indeed, if the refraction at an interface is negative, the refracted transmission will be deflected towards the same side as the incident wave with respect to the normal of the interface. Such an unusual deflection can give rise to a focused image when waves pass through a rectangular slab. This negative refraction scenario is illustrated by Fig. 1(b2).

There is ambiguity in the explanation of the apparent focusing effect in the context of negative refraction. As indicated in Fig. 1(b2), if the focused image were caused by a negative refraction, particularly when the negative refraction is all angle, a focused point would also prevail inside the slab, according to Fig. 1(b2). The expected focused image, however, is noticeable neither in the previous simulations, nor in our simulations. Here, we note that the image field inside the slab, shown in Figs. 1(c) and 1(d), is not clear. It is hard to see whether there is a focused image inside the slab, because the slab is small; we have purposely used the small slab, so as to be more comparable with the simulation in Ref. [9]. In the following, we will use large sample sizes, so that the fields inside the samples can be visualized better.

When we further explore the focusing effect shown on the other side of the slab, we find that such a focusing effect does not have to be explained as the occurrence of negative refraction. Rather, it is purely due to the nature of some band structures. The band structure from Fig. 1(a) clearly shows that in the frequency range considered, there is a band gap along the ΓX direction, i.e., the [1,0] direction. Therefore, the waves are prohibited from propagation along this direction. In other directions such as ΓM, however, there is an allowed band to support the propagation of waves. In the present setup, as well as in previous setups, the incident wave is set along the ΓM direction, which makes an angle of 45 degrees to the ΓX direction. As they are prohibited from propagating in the ΓX direction, i.e., 45 degrees from the straight horizontal direction, waves naturally tend to move forward along the ΓM direction. The frequency band in the ΓM direction provides a propagating avenue for the waves to go over to the other side of the slab, like a gas pipeline or a water tap. To put our discussion into perspective, we have done a variety of simulations. Some of the key results are shown below.

Figure 2 shows the imaging fields with a larger rectangular slab. All the parameters are taken as the same as that in Fig. 1, except that the thickness of the slab has been increased to $10\sqrt{2}$, allowing us to study the nature of wave propagation inside the slab for the reasons stated above. The overall fields are imaged in (a1) and (a2) in terms of the real part and the modulus of the electric field, respectively. The fields within the slab have been purposely zoomed and replotted in (b1) and (b2) for the sake of clarity. Figure 2(a1) clearly shows a focused image across the slab. Within the slab, it is clearly shown by (a2), (b1), and (b2) that the transmission is mainly focused within a pipeline or tunnel along the ΓM direction. When plotting in real time, such a guided transmission is more beautifully presented. This feature is fully in accordance with the above discussion of the expected properties of the band structure that has a partial gap. The apparent focused image across the slab is in fact just the outburst point of the transmitted waves. Simply, the pass band in the ΓM acts as a transportation carrier that moves the

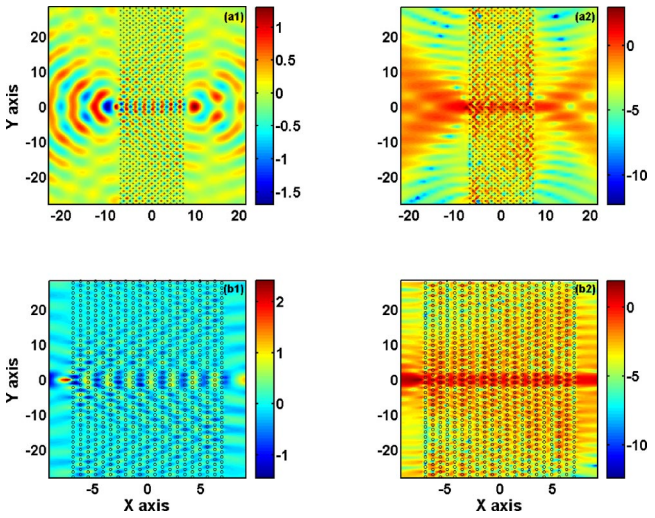

FIG. 2. (Color online) The imaging fields for a slab of photonic crystal structure, similar to Fig. 1 but with a larger sample length. (a1) and (b1) show the real part of the field, (a2) and (b2) show the intensity field. (b1) and (b2) are replots of the imaging fields for the area inside the slab from (a1) and (a2), respectively. Here we see clearly that the waves propagate in a small tunnel inside the slab; it is most evident in (b2).

source to the other side of the slab. The waves on the right-hand side of the slab look as if they were radiated by an image that has been transported across the slab within a narrow guide. If such an imaging phenomenon had to be interpreted in the framework of an effective medium theory without worrying about what is really going on inside the medium, the negative refraction would be one of the options to be resorted to. But the present results suggest that this is not a correct explanation.

To further support our observation, we place a transmitting source *inside* an array of cylinders. The overall shape of the array is square. Figure 3 presents the simulation results. Again, all the parameters for the physical quantities are taken from Fig. 1. The cylinders are arranged to form a square

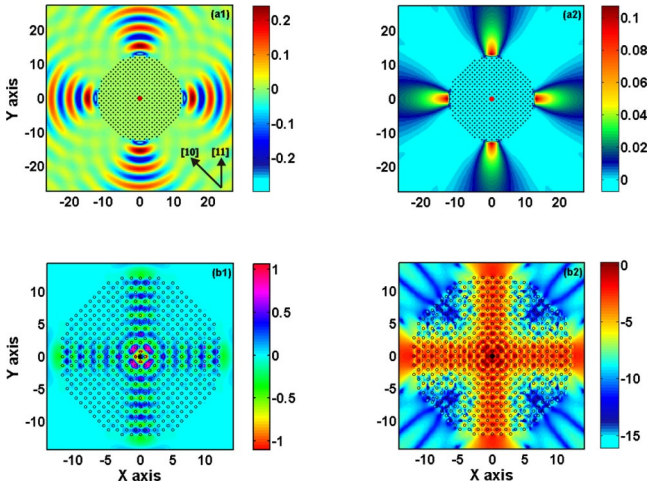

FIG. 3. (Color online) The imaging fields for a transmitting source located inside a square array of cylinders. The square measures $14\sqrt{2}\times 14\sqrt{2}$. All other parameters are the same as in Fig. 1.

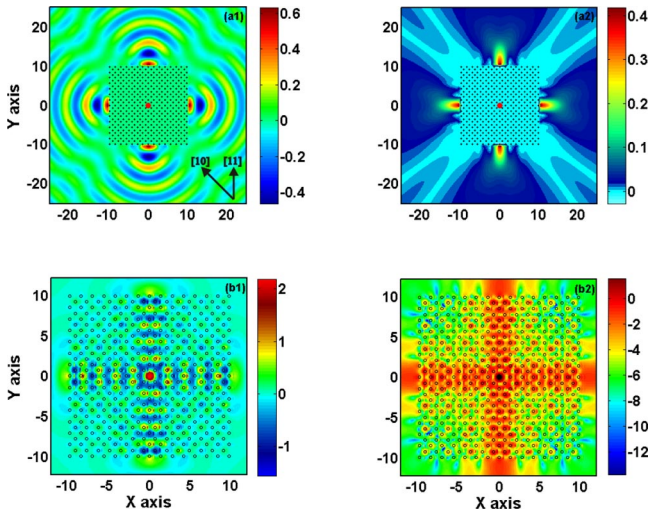

FIG. 4. (Color online) The imaging fields for a transmitting source located inside a roughly circularly shaped array of cylinders. The total number of cylinders is 484. All other parameters are the same as in Fig. 1.

crystal inside a square area whose side measures $14\sqrt{2}$. The geometry of the setup can be seen in Fig. 3. Here, to show the results in their most explicit form, we plot separately the fields within and outside the photonic crystal structure. Figure 3(a1) and 3(a2) show the real part and the modulus of the electric field outside the array of the cylinders, whereas Figs. 3(b1) and 3(b2) show the real part and the modulus of the electric field inside the array of the cylinders. As expected, the focused images are evident in four allowed directions, in the $[1,1]$, $[-1,1]$, $[-1,-1]$, and $[1,-1]$ directions, respectively, as shown by (a1) and (a2). The images of the field inside the array clearly show the traveling path of the waves along these directions, depicted by (b1) and (b2).

We have also considered the situation in which we place the transmitting source inside an array of cylinders and the array takes roughly a circular shape. The results are shown in Fig. 4. Again, if the effectively negative refraction or all-angle negative refraction exists, the waves are expected to propagate in all directions—no focusing should be expected. The results indicate that this is untrue. Similar to Fig. 3, the geometry of the setup can be seen in Fig. 4. The fields within and outside the photonic crystal structure are plotted separately. Figures 4(a1) and 4(a2) show the real part and the modulus of the electric field outside the array of the cylinders, while Fig. 4(b1) and 4(b2) show the real part and the modulus of the electric field inside the array of the cylinders. Here we also observe the focused images as in the case of Fig. 3. These images are in the $[1,1]$, $[-1,1]$, $[-1,-1]$, and $[1,-1]$ directions, respectively, as shown by (a1) and (a2). Inside the arrays, the waves clearly travel along these directions, depicted by (b1) and (b2). By comparing Fig. 3 and Fig. 4, we conclude that the imaging feature and wave propagation are insensitive to the outer shape of the arrays, i.e., the boundary of the photonic crystals.

All the imaging effects shown so far can be well explained in terms of the band-structure properties. We have

also considered other frequencies both inside and outside the shaded area of Fig. 1(a). We observe that the field patterns are qualitatively similar. But when the frequency moves towards the edge of the partial band gap in the ΓX direction, the apparent guided propagation inside the photonic crystal tends to diminish, leading to a gradual disappearance of the "focusing" effects. This is reasonable. As the frequency moves towards the edge of the forbidden band of the ΓX direction, the waves would be either allowed to propagation in all directions or forbidden to travel in all directions due to the complete band gap located just above the first frequency band. Therefore the imaging effect caused by the partial band gap diminishes.

In summary, we have considered the optical transmission in a photonic crystal. The results show that the imaging effect which has been previously interpreted as a signature of the negative refractive effects is caused by tunneling or guided propagation in the presence of partial band gaps. The refraction need not be interpreted as being negative. After we submitted this paper, Li and Lin reported a similar observation [19].

This work received support from NSC and NCU. The early participation of Ken Kang-Hsien Wang is greatly appreciated. One of us (C.K.) is particularly grateful to him for many inspiring discussions and help.

[1] V. G. Veselago, Sov. Phys. Usp. **10**, 509 (1968).
[2] A. L. Pokrovsky and A. L. Efros, Phys. Rev. Lett. **89**, 093901 (2002).
[3] G. W. van 't Hooft, Phys. Rev. Lett. **87**, 249701 (2001).
[4] J. M. Williams, Phys. Rev. Lett. **87**, 249703 (2001).
[5] P. M. Valanju, R. M. Walser, and A. P. Valanju, Phys. Rev. Lett. **88**, 187401 (2002).
[6] N. Garcia and M. Nieto-Vesperinas, Phys. Rev. Lett. **88**, 207403 (2002).
[7] Z. Ye, Phys. Rev. B **67**, 193106 (2003).
[8] C. Luo, S. G. Johnson, J. D. Joannopoulos, and J. B. Pendry, Phys. Rev. B **65**, 201104(R) (2002).
[9] S. Foteinopoulou, E. N. Economou, and C. M. Soukoulis, Phys. Rev. Lett. **90**, 107402 (2003).
[10] R. A. Shelby, D. R. Smith, and S. Schultz, Science **292**, 77 (2001).
[11] A. A. Houck, J. B. Brock, and I. L. Chuang, Phys. Rev. Lett. **90**, 137401 (2003); C. G. Parazzoli, R. B. Greegor, K. Li, B. E. C. Koltenbah, and M. Tanielian, *ibid.* **90**, 107401 (2003).
[12] H. Kosaka, T. Kawashima, A. Tomita, M. Notomi, T. Tamamura, T. Sato, and S. Kawakami, Phys. Rev. B **58**, R10096 (1998).
[13] J. A. Kong, B. I. Wu, and Y. Zhang, Appl. Phys. Lett. **80**, 2084 (2002).
[14] V. Twersky, J. Acoust. Soc. Am. **24**, 42 (1951); J. Math. Phys. **3**, 700 (1962).
[15] D. Felbacq, G. Tayeb, and D. Maystre, J. Opt. Soc. Am. A **11**, 2526 (1994).
[16] Y.-Y. Chen and Z. Ye, Phys. Rev. Lett. **87**, 184301 (2001).
[17] H. Kagemoto and D. K.-P. Yue, J. Fluid Mech. **166**, 189 (1986).
[18] B. Gupta and Z. Ye, J. Appl. Phys. **94**, 2173 (2003).
[19] Z.-Y. Li and L. Lin, Phys. Rev. B **68**, 245110 (2003).